Int. J. Multiphase Flow Vol. 13, No. 5, pp. 649–660, 1987
Printed in Great Britain.

0301-9322/87 $3.00 + 0.00

BUBBLE FORMATION IN A SINGLE-JET GAS–SOLID FLUIDIZED BED

X.-R. ZHANG,† G. M. HOMSY and W. T. ROPCHAN‡
Chemical Engineering Department, Stanford University, Stanford, CA 94305, U.S.A.

(*Received* 4 *August* 1986; *in revised form* 24 *December* 1986)

Abstract—The jet instability and bubble frequencies in a single-orifice 2-D gas–solid fluidized bed were studied by flow visualization and measured by means of a high-sensitivity capacitance probe. The influence of a series of parameters, including particle size (0.105–0.590 mm), particle density (590–3990 kg/m^3), probe vertical location, jet flow rate (0.5×10^{-4}–35×10^{-4} m^3/s) and background gas flow rate (0–4 times minimum fluidization velocity), on the bubble frequency was investigated. For the smallest particle size studied, the jet instability frequency was in good agreement with a 2-D version of a simple model due to Davidson and Harrison. The data show a systematic deviation from that model for increasing particle size. The model is then modified to account for the fact that with large particles, gas leakage from the forming bubble to the surrounding emulsion phase becomes important. The modified leakage model agrees well with the experimental data. Bubble coalescence at the tip of the jet was shown to result in bubble frequencies which are simple subharmonics of the basic pinching frequencies of the jet.

1. INTRODUCTION

The phenomenon of bubble formation from jets entering a fluidized bed is important in many applications. In the case of fast chemical reactions, perhaps involving volatilization reactions, the fluid mechanics of jet formation and instability can have a controlling influence on conversion in the grid region. Even for relatively slow reactions, the phenomena there will influence the initial bubble size distribution which in turn may have a strong influence on the evolution of the bubble population. As an extreme example, some reactor configurations involve a very large jetting region surrounded by an annular zone in which chemical conditions different from those in the jet may be maintained. Thus, for a variety of reasons, the study of jets and jet break-up is important.

Much of the work on jets has been summarized recently by Massimilla (1985). While much of the literature has been concerned with certain time-averaged quantities, e.g. the average turbulent velocity profiles in the jet, the average penetration height of a jet etc., relatively few systematic studies of the dynamic behavior of jets have been reported. Although there are many points of disagreement in the literature, the following broad generalizations may be made. As gas enters into a bed of particles, it penetrates some vertical distance before breaking up into bubbles. There seem to be a wide variety of instability modes involved in this break-up process, ranging from a discrete chain of bubbles issuing from the orifice, through the disengagement of a bubble from the tip of a plume-like structure, to a more complicated mode of chaotic bubble shedding from a flame-like structure. Most of these modes are summarized and discussed by Massimilla (1985), who points out that no general picture of the conditions under which one or the other mode may occur is available. There have also been observations and measurements of the frequency of bubble formation as a result of the break-up of the jet, typified by Rowe *et al.* (1979), Sit & Grace (1981) and Yang *et al.* (1983, 1986). Many of these more quantitative studies have been made over restricted ranges of particle size and flow rate, but again a few general observations may be made. First, the mode of instability may depend upon whether the particles are aerated, perhaps even incipiently fluidized, or not, with the break-up at the top of a jet-like plume being more easily observed with aeration. However, the frequency of bubble formation seems relatively insensitive to the mode of break-up (Sit & Grace 1981). Second, the bubble frequency depends on the occurrence of significant coalescence between bubbles, which in turn can depend upon the mode

†‡Present addresses: †Shanghai Petrochemical Complex, Foreign Contract Department, Shanghai, People's Republic of China; ‡Air Products & Chemicals Inc., Allentown, Pa, U.S.A.

of break-up, and can also depend upon the degree to which gas leaks from the jet into the surrounding emulsion phase. Finally, simple models (discussed below) which predict the bubble frequency can be substantially in error, probably as a result of coalescence and leakage. Again, very few studies have attempted to quantify the effect of either the coalescence or leakage.

There have been very few quantitative models of the mechanics of bubble formation at an orifice or at a source of gas. The best known is that given in Davidson & Harrison (1963, Chap. 3). In this model, the details of which will not be repeated here, the shape of the bubble is taken to be a spherical section, and the basic force balance describing the acceleration of this buoyant sphere equates the buoyant force of the sphere to that required to inertially accelerate the emulsion phase around the bubbles. The balance of these forces then establishes a time scale from which a bubble frequency may be determined; the model specifically excludes loss of gas to the emulsion phase, which implies that conservation of mass determines the kinematics of the motion. The result for the bubble frequency is the widely quoted relationship

$$f = \left(\frac{\pi g^3}{6Q}\right)^{1/5}, \qquad [1]$$

where g is the gravitational constant and Q is the volumetric flow rate. Davidson & Harrison (1963) discuss factors which may influence the numerical constant, $(\pi/6)^{1/5}$, in this relation, but the basic scalings are established simply from the forces involved. Any phenomena involving a balance of buoyancy and particle inertia will exhibit this basic time scale.

Zenz (1971) has criticized the simple Davidson–Harrison model on the grounds that in many cases, the flow regime is such that the shape of the bubble–jet combination is far from that assumed in the model, and that leakage is a dominant effect at high flow rates. Recently, Caram & Hsu (1986) have considered an extension of the model, in which leakage is specifically accounted for. Assuming that the leakage rate is always at u_{mf}, they find that the bubble frequency differs from that given by [1] as a dimensionless leakage rate, $(u_{mf}^5/g^2Q)^{1/3}$, increases, with the frequency increasing with increasing leakage, as expected.

It is a simple matter to repeat the analysis for a 2-D bed, in which the shape is taken to be a cylinder instead of a sphere. The resulting expression, under the same assumptions, is (Ropchan 1981)

$$f = \left(\frac{\pi}{16}\frac{g^2 d}{Q}\right)^{1/3}, \qquad [2]$$

where d is the thickness of the bed. The expression in [2] can be similarly modified in order to account for gas leakage from the cylindrical 2-D bubble. In a short study, Nguyen & Leung (1972) measured both bubble frequency and bubble area during bubble formation at an orifice in a 2-D fluidized bed operated at $u = 1.5\,u_{mf}$. They found under these conditions of fixed flow rate and fixed particle size that approx. 50% of the entering gas leaked into the emulsion phase, with a corresponding increase in the frequency of approx. $2^{1/3}$. Their data show a $Q^{-1/3}$ dependence of frequency on flow rate, but with a systematic negative deviation from the modified form of [2]. Finally, Yang *et al.* (1983) have considered a model of 2-D bubble formation which includes leakage, but did not integrate the equation of motion of the bubble to obtain a prediction of bubble frequency.

The objectives of the present work, then, are to make observations of the flow regimes and instability modes of jets, as well as measurements of bubble frequencies and coalescence statistics over as wide a range of flow rates and particle sizes as possible, in order to understand the *dynamics* of the bubble formation process.

2. EXPERIMENTAL METHOD

Apparatus

A diagram of the experimental apparatus and the data acquisition system is shown in figure 1. Experiments were performed in a conventional 2-D fluidized bed of cross section 292 × 16 mm. Flow distribution was accomplished by an air manifold which issued into a calming section. The main test section was 914 mm high and the construction was of Plexiglas. The inner walls were

treated with plastic contact sheets and the air was humidified in order to reduce the effect of electrostatic charge. Air was filtered following the humidifier and flow measured by flowmeters. Two separate streams of gas, one for the main jet, the other for the background, were allowed for. Between the calming section and the main test section there was a piece of sintered stainless-steel porous plate, 1 mm in thickness, as a gas distributor which was divided into two parts by a compartment underneath. The center part, 13 × 16 mm, was for jet gas to form bubbles and the outer part on both sides of the orifice was for background gas feeding to maintain the bed materials in the minimum fluidization state.

Techniques

In addition to visual observation by eye of the behavior in the grid region, two different techniques were used to obtain permanent visual records of the events taking place. Cinephotography, at a calibrated filming speed of 56 frame/s, was done with a 16 mm movie camera (Bolex H-16 Rex) on black-and-white film. In addition, still photographs were taken with a 35 mm camera (Canon FTR) on high-contrast black-and-white film.

The data acquisition system consisted of a high-sensitivity capacitance probe with a novel circuit, a sine-wave generator, a signal amplifier, a strip chart recorder, an oscilloscope, a real-time spectrum analyzer and a digital averager (Honeywell, Model SA1-51C) and an X–Y recorder. We

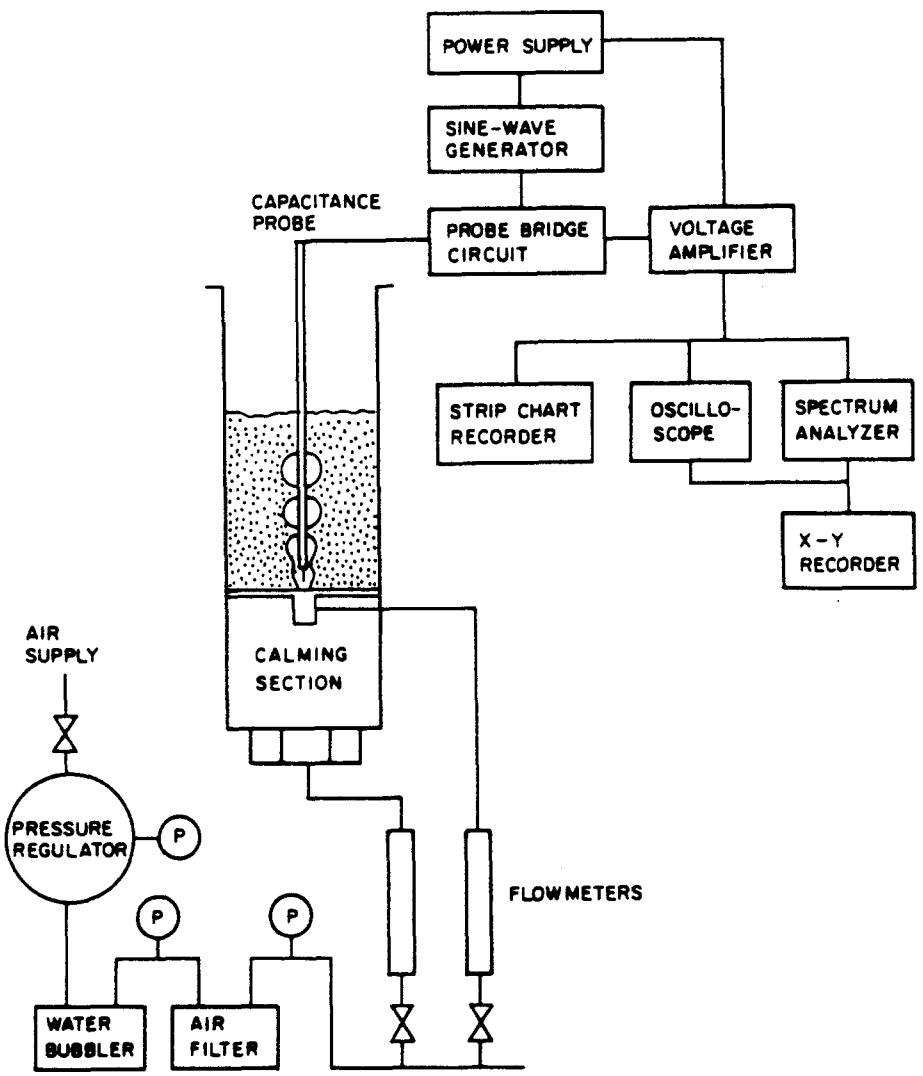

Figure 1. Schematic of the apparatus.

utilized a high-sensitivity capacitance probe, designed by Fitzgerald (1983), which eliminates the problem of probe lead length, a problem commonly encountered in capacitance-type bubble detectors. The rod-type probe was made of two wires tipped with a mini-diode and a 10 MΩ resistor fitted on top of a copper cylindrical tube of 3 mm o.d. The probe is designed to resolve capacitance changes of a few femtofarads. A bridge circuit was employed to detect the signals which were then amplified and fed into a real-time spectrum analyzer and digital averager to obtain the power spectrum over the range 0–20 Hz. The power spectrum was displayed on the oscilloscope and recorded on an $X-Y$ recorder. As will be discussed below, the peak frequency on the power spectrum plot corresponds under some conditions to the bubble formation frequency. The data thus obtained were checked with a frame-by-frame analysis of the films. Good agreement between the two approaches proved the effectiveness of the capacitance probe method.

Variables

The experimental variables under investigation were jet flow rate, background gas flow rate, initial fixed bed height, probe vertical location, particle size and particle density. In table 1, the properties of the particles used in the study are listed: note the wide range of particle densities used. Not all particles were used in all experiments. The range of jet air flow rate was 50×10^{-6}–3450×10^{-6} m^3/s, corresponding to a jet superficial velocity of 0.24–16.60 m/s.

3. EXPERIMENTAL RESULTS

Flow visualization

The first experimental work consisted of visualization studies. As a representative sample, the results for one particular particle (type 4) will be discussed. Observations were first made in the grid region as the air supply flow rate was increased. The start of the jet regime occurred at a flow rate of 546 cm^3/s, the first of which is characterized by a jet whose orientation is vertical, and which periodically breaks up into bubbles. At $Q = 966$ cm^3/s, the jet could be said to have lost its stationarity, i.e. it now meanders from side to side with no apparent regularity or preferred position. At $Q = 1373$ cm^3/s the jet definitely became irregular in shape, but fixed in position once again, and virtually continuous from the orifice well into the bed. Figure 2 shows typical still photographs of these regimes of jet behavior. These regimes are typical of what has been seen before, ranging from the periodic pinching of a vertical jet to form bubbles at low flow rates [see, for example, Sit & Grace (1981)] to the more sinuous "flame-like" structures which occur at high flow rates (Zenz 1968).

Quantitative analysis of films

Because of the complexity of the phenomena involved, the quantitative studies were confined to the first regime of flow.

From slow playback of the cine visualizations, it it clear that a rather elongated bubble in the shape of a jet first pinches off just above the orifice. This pinching was quite reproducible for a given particle type and air flow rate. The pinching frequency, determined by a frame-by-frame analysis, is shown in figure 3, together with the simple relation [2]. It is seen that this frequency

Table 1. Physical properties of particles

No.	Type	Particle size range, d (mm)	Particle density, ρ_s (kg/m^3)	Minimum fluidization velocity, u_{mf} (m/s)
1	Silica gel	0.105–0.149	590	0.0072
2	Silica gel	0.074–0.250	1620	0.021
3	Microbeads[a]	0.177–0.210	2990	0.060
4	Microbeads	0.25–0.297	2990	0.12
5	Microbeads	0.350–0.420	2990	0.37
6	Microbeads	0.500–0.590	2990	0.48
7	Microbeads	0.42–0.59	3990	0.6

[a]Cataphote microbeads.

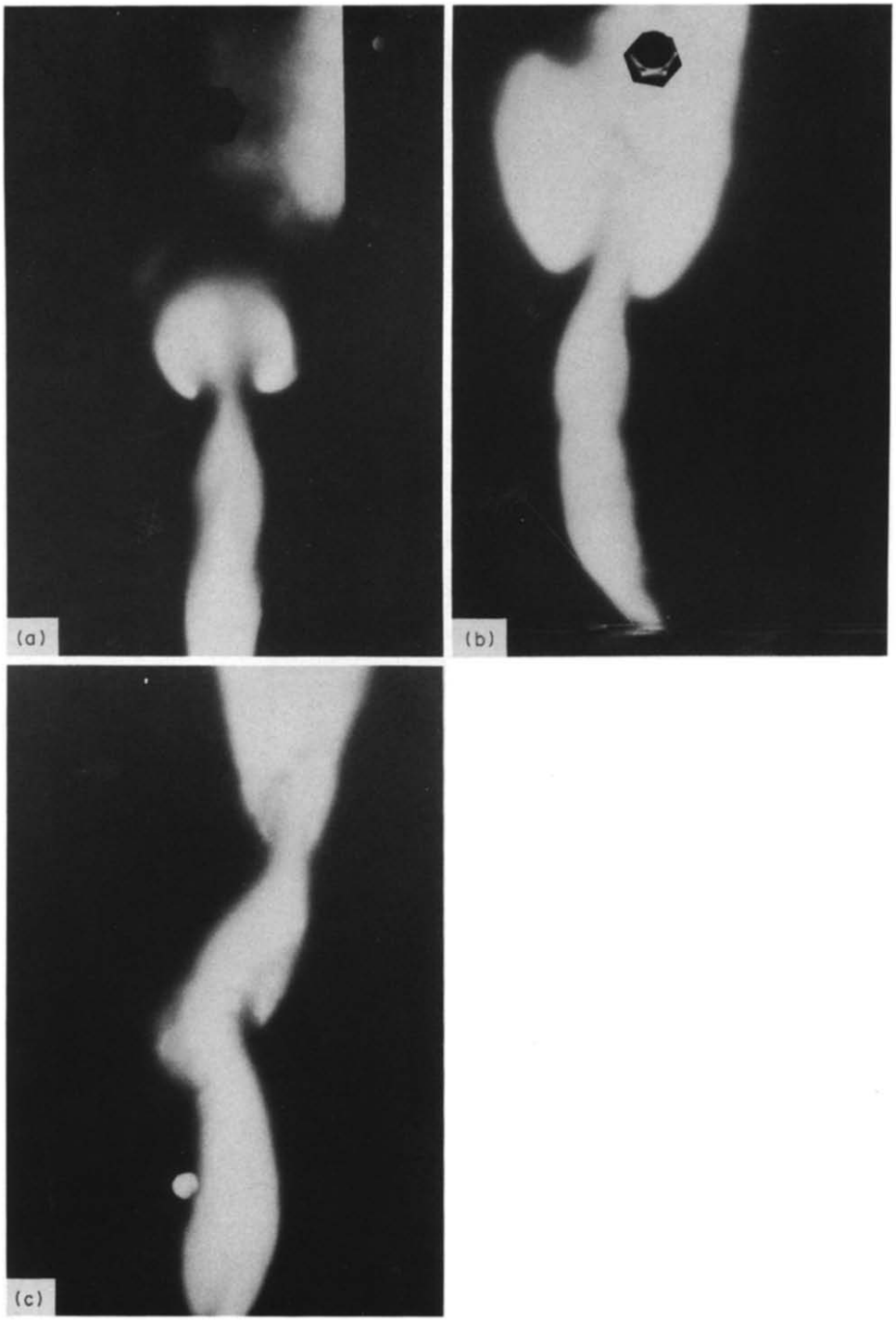

Figures 2a–c. Photographs of the three regimes of jet behavior.

Table 2. Coalescence statistics

Particle type	Singlet bubble (%)	Doublet bubble (%)	Triplet bubble (%)	Quadruplet bubble (%)
3	0	47	47	6
4	3	47	45	5

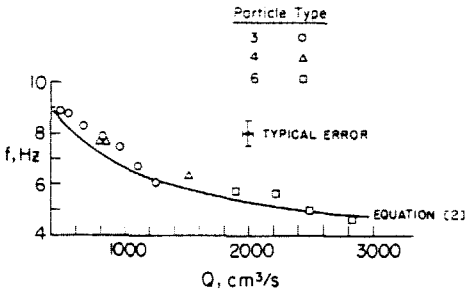

Figure 3. Jet pinching frequencies from visualizations.

is largely independent of particle size and density over the range studied here, and is primarily a function of gas flow rate. It is also seen that there is a small but consistent positive deviation of the data from [2]. This will be shown later to be due to gas leakage from the jet. The height at which this pinching off occurred varied slightly with flow rate for all particle types, from < 1.4 cm above the base of the bed (i.e. below the upper edge of the bottom flange of the test section) for particle types 3 and 4, to 3–5 cm for particle types 6 and 7. Further analysis of the filmed observations showed that the pinched-off bubble itself forms into conventionally-shaped 2-D bubbles, which coalesce into doublets, triplets etc. These bubbles, in turn, were found to rise, split and coalesce, as do those in conventional gas fluidized beds. The fate of the structure formed after pinching is of great interest, as it determined the bubble size and frequency in the immediate vicinity of the grid. A frame-by-frame analysis was done for several sequences in order to obtain the statistics of bubble formation following jet break-up. It was found that very few, if any, of these structures moved away as single bubbles, and coalescence phenomena dominated the resulting bubble frequency. Thus we draw a distinction between the basic instability frequency of the jet, referred to as the "pinching frequency", and the resulting bubble frequency. In previous studies of single bubble formation at an orifice, these are often equal, but in a jet they are not. Typical overall coalescence statistics from two film sequences are given in table 2. The most notable observation was the lack of an apparent preference for the type of bubble formed, but that doublets and triplets dominate the statistics. Furthermore, a detailed analysis of the pattern of events showed that this was random in the sense that each structure coalesced or not, independently of what had gone before. This tendency for bubbles, once formed, to coalesce, has not been studied in great detail before, and, as will be shown below, is the probable cause for measured bubble frequencies to be substantially below those predicted by [2] or its 3-D analogue. This point of view is in agreement with the observations of Yang *et al.* (1983, 1986).

Capacitance probe studies

A typical trace of an amplified bridge voltage imbalance is shown in figure 4 in which the pinching frequency is clearly visible, and its corresponding averaged power spectra plot in figure 5. The effect of different averaging intervals on the power spectrum plots at the same operating conditions was studied. It was found that as the averaging is increased, the spectra tended to become smoother, but the major peaks remain unaltered. In this research all power spectrum plots were done with 64 averages, and the corresponding analysis time was 10 min 40 s. The selected frequency test range was 0–20 Hz. Typical peak frequency error was 0.5 Hz.

Two types of frequency spectra were observed which consisted of single-peaked and multipeaked patterns. Figures 6a, b show typical double-peak and triple-peak spectra, implying the existence

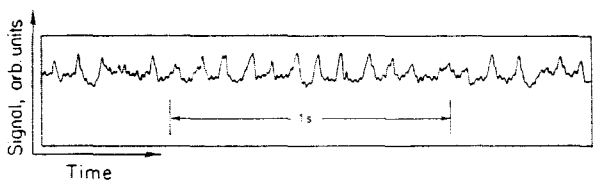

Figure 4. Typical capacitance probe trace—particle type 1, $Q = 4 \times 10^{-4}$ m³/s, probe height = 1 mm.

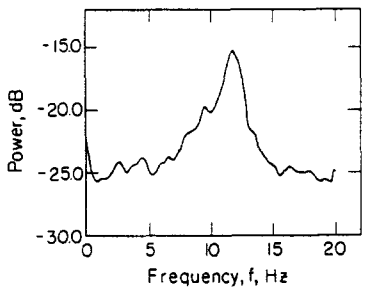

Figure 5. Power spectrum corresponding to figure 4.

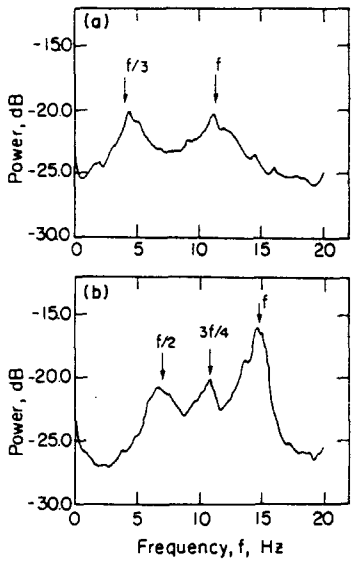

Figure 6. Typical spectra in the region of coalescence—particle type 3, probe height 10 mm: (a) $Q = 9.1 \times 10^{-4}$ cm^3/s; (b) $Q = 2.4 \times 10^{-4}$ cm^3/s.

of two or three major frequencies because of bubble coalescence. Normally, in the case of double-peaked spectra, the lower-frequency peak had a frequency $1/2 \sim 1/3$ of that for the higher-frequency peak. An example of this is shown in figure 6a. Figure 6b, corresponding to a lower flow rate than figure 6a, exhibits a $3f/4$ peak as well as an $f/2$ peak: the reasons for this behavior are presumably that at this flow rate, the probe is located in the region of complex motion corresponding to coalescence (see also figure 11). The more familiar pattern was an evolution of the primary pinching frequency to an $f/2$ or $f/3$ peak.

Before discussion the quantitative results in detail, we will briefly comment on the effect of bed depth and background gas flow on the phenomena discussed below. The bed depth was varied over a substantial range, and it was found that as long as the depth was 2–3 times the maximum jet penetration depth, the depth had no appreciable effect on the jet or bubble frequency. This is entirely expected, and indicates that the phenomena measured were characteristic of deep-bed behavior.

The effect of background gas was also studied. The background gas flow was varied form 0 to $4 \times u_{mf}$. Above $1 \times u_{mf}$, there is, of course spontaneous bubbling in the regions removed from the jet, with behavior more akin to uniformly bubbling beds. For flow rates between 0 and $1 \times u_{mf}$, we found that the coupling between the jet flow and the emulsion phase was weak, with no substantial modification of the basic instability modes of the jet. Virtually all of our conclusions are valid for the case in which there is background gas. An example of this is illustrated in figure 7, where the position of the spectral peak is unchanged, but its intensity diminishes somewhat as the background gas velocity is increased. These observations are in agreement with those of Sit (1981), who reported that over a very limited range of flow rate, the pinching frequency was unaltered by the presence of background gas. Thus, the remainder of the data discussed are for the case of no background gas.

An extensive set of measurements of pinching frequencies was made, varying both particle size and flow rate, keeping the axial location of probe fixed. Figures 8–10 give the results of this study. Results for particle types 2 and 3 were similar to those for type 1. This illustrates that particle density is unimportant in determining the pinching frequency, in agreement with the model described below. For the smallest particles studied, there is generally good agreement between the data and the simple relation [2]. However, as particle size increases, there is a systematic positive deviation of the data from [2]. This deviation is explained below, where we develop an improved version of the model on which [2] is based. Also notice that in some circumstances, there are two frequencies for a given flow rate, indicating the existence of double-peaked spectra, as in figure

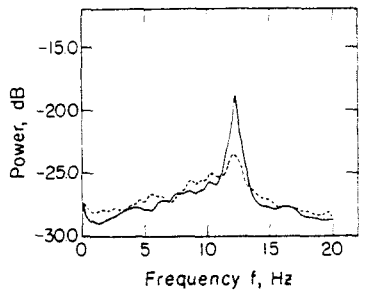

Figure 7. The effect of background gas on pinching frequency—particle type 3, $Q = 5 \times 10^{-4}$ cm^3/s: ——, no background gas; – – –, background gas at u_{mf}.

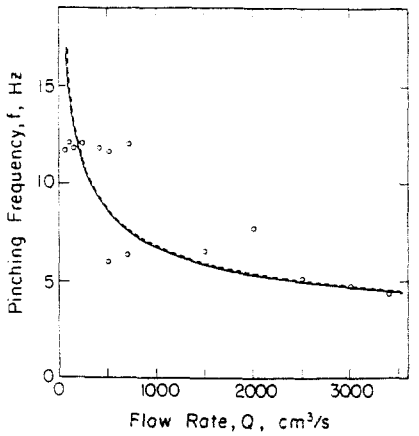

Figure 8. Pinching frequency as a function of flow rate—particle type 1: ——, [2]; – – –, numerical solution of [11].

6a. We are unsure if this corresponds to a change in flow regime or a coincidence of the probe location and the region of bubble coalescence, but further visualization studies may be required to settle the issue.

Since the phenomena of bubble coalescence leads to a shift in the dynamical quantities with axial position, we undertook a study in which axial traverses of the probe were performed. As expected from the well-known bubble coalescence phenomenon, bubble frequency decreases as bubbles rise from the tip of the jet. Figure 11 demonstrates the evolution of the power spectra with bed height at constant flow rate. Note the shifting of the main peaks from higher frequency to lower frequency as a result of bubble coalescence along the bed height. As noted above, the region of significant coalescence is approx. 20–30 mm above the distributor, which in this case, results in $f/2$ and $f/3$ peaks, indicative of doublet and triplet coalescence. The further evolution of the $f/3$ peak with height is due to a number of factors, including lateral coalescence with other bubbles present at these heights, and leakage of gas into the emulsion region. Such an evolution is similar in many respects to that observed by Yang *et al.* (1986), although they do not discuss the reasons for it.

4. MODEL

From the experimental data so far we have gathered that the bubble formation frequency for a single jet in a 2-D gas–solid fluidized bed is a function of jet gas flow rate and is affected by particle size and perhaps by density. Furthermore, we notice for large particles a systematic positive deviation in the frequency from that predicted by a simple model which ignores the interaction

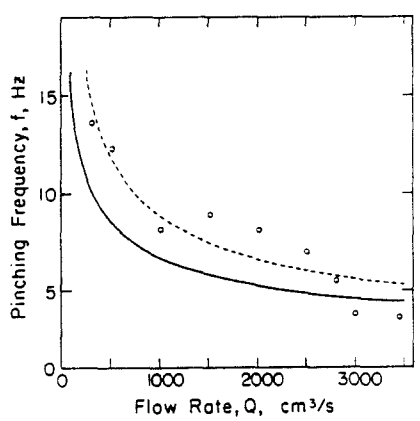

Figure 9. Pinching frequency as a function of flow rate—particle type 5: ——, [2]; – – –, numerical solution of [11].

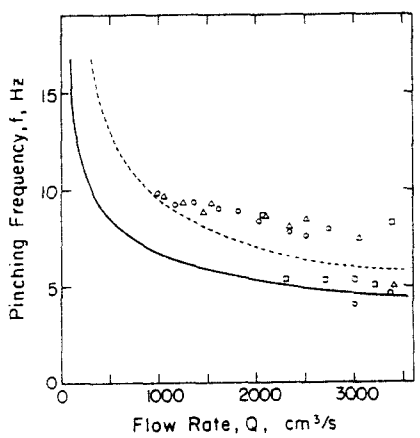

Figure 10. Pinching frequency as a function of flow rate—particle type 6: ——, [2]; – – –, numerical solution of [11].

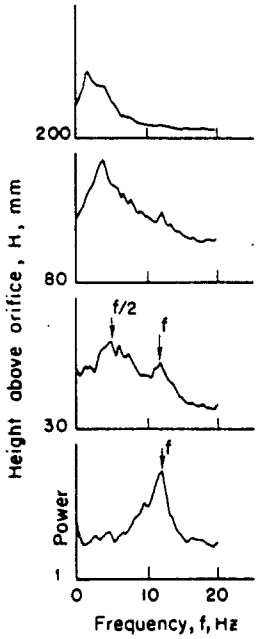

Figure 11. Typical axial traverse showing the evolution of the spectra from jet pinching through coalescence to bubbling.

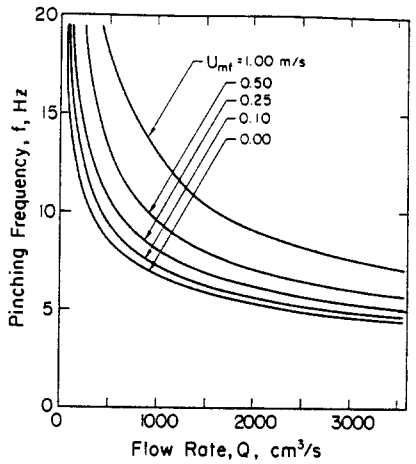

Figure 12. Pinching frequency as a function of flow rate, with gas leakage velocity, u_{mf}, as a parameter.

between jet gas and the emulsion phase. In order to improve upon that simple model, one which allows for leakage from the jet to the emulsion is developed below.

The basic assumptions for the leakage model are:

(1) the emulsion phase of the fluidized bed behaves as an inviscid fluid;
(2) the bubble is cylindrical in form;
(3) the net leakage from a forming bubble into the surrounding emulsion phase occurs only on the top hemicircle of the bubble;
(4) the net gas leaking velocity from the bubble to the emulsion phase is equal to the minimum fluidization velocity, u_{mf}.

The last three of these assumptions are somewhat arbitrary, but we do not attempt here to solve the free-boundary problem of the shape of a jet entering a fluidized bed. Thus, assumptions of the model such as a radially directed velocity over only half of a circle are made only to establish trends and the correct order of magnitude of the effect. Various refinements of these assumptions do not seem warranted at this time.

Consider a bubble during its formation but prior to detachment from the orifice opening. Because of buoyancy, after time t, the bubble center has risen a distance S. If the jet gas flow rate is constant from the orifice, the bubble volume V_b at any time is given by the mass balance equation

$$V = Qt = V_b + V_l, \qquad [3]$$

where V is the total gas volume, Q is the gas flow rate at the orifice, t is the time, V_b is the bubble volume and V_l is the volume of gas leaked from the bubble to the surrounding emulsion phase. According to the assumptions of the model,

$$V_b = \pi r^2 d \qquad [4]$$

and

$$V_l = \pi r d\, u_{mf} t, \qquad [5]$$

thus

$$dV = Q\,dt = dV_b + dV_l \qquad [6]$$

$$2\pi dr\frac{\mathrm{d}r}{\mathrm{d}t} = (Q - \pi d\, u_{\mathrm{mf}}\, r). \qquad [7]$$

On integrating [7] and assuming $r = 0$ at $t = 0$.

$$t = \frac{2}{u_{\mathrm{mf}}}\left[\frac{Q}{\pi d u_{\mathrm{mf}}}\ln\left[\frac{\dfrac{Q}{\pi d u_{\mathrm{mf}}}}{\dfrac{Q}{\pi d u_{\mathrm{mf}}} - r}\right] - r\right]. \qquad [8]$$

Equation [8] is an implicit expression for the bubble radius as a function of time. It is assumed that the bubble will detach when its base reaches the orifice opening, i.e. when $r = S$ the bubble will detach. A similar relation was used by Yang *et al.* (1983), in order to infer the effect of gas leakage on bubble size. However, since it is only a kinematic relation, it cannot be used to predict the frequency. The quantity S, and therefore the frequency, can be calculated from the mechanics of the upward motion of the bubble.

The coefficient of virtual mass for a cylinder is unity. Thus, the upward momentum of the emulsion phase surrounding the forming bubble is $\rho_b V_b \mathrm{d}S/\mathrm{d}t$. The upward motion of the bubble is determined by balancing the buoyancy force of the bubble $\rho_b V_b$ against the rate of change of upward momentum of the emulsion phase surrounding the forming bubble, the inertia of the air within the bubble being neglected:

$$\frac{\mathrm{d}}{\mathrm{d}t}\left(\rho_b V_b \frac{\mathrm{d}S}{\mathrm{d}t}\right) = \rho_b V_b g, \qquad [9]$$

with the initial conditions being

$$t = 0, \quad r = 0, \quad S = 0, \quad \frac{\mathrm{d}S}{\mathrm{d}t} = 0. \qquad [10]$$

Upon substitution of [8] into [9] and changing variables we have,

$$\frac{\mathrm{d}}{\mathrm{d}r}\left[\frac{u_{\mathrm{mf}} r}{2}\left(\frac{Q}{\pi d u_{\mathrm{mf}}} - r\right)\frac{\mathrm{d}S}{\mathrm{d}r}\right] = \frac{\dfrac{2gr^3}{u_{\mathrm{mf}}}}{\dfrac{Q}{\pi d u_{\mathrm{mf}}} - r} \qquad [11]$$

and the corresponding initial conditions,

$$r = 0, \quad S = 0, \quad \frac{\mathrm{d}S}{\mathrm{d}r} = 0. \qquad [12]$$

Equation [11] is a non-linear second-order differential equation for $S = S(r)$ which cannot be solved to obtain an analytical expression but can be solved numerically. By evaluating [8] at $r = r_b$, for which $t = t_b$, the time needed to issue the bubble is

$$t_b = \frac{2}{u_{\mathrm{mf}}}\left[\frac{Q}{\pi d w u_{\mathrm{mf}}}\ln\left[\frac{\dfrac{Q}{\pi d u_{\mathrm{mf}}}}{\dfrac{Q}{\pi d u_{\mathrm{mf}}} - r_b}\right] - r_b\right]. \qquad [13]$$

The bubble formation frequency f is simply $1/t_b$.

Equations [11]–[13] were solved numerically to obtain the bubble frequency f at different jet flow rates Q and different minimum fluidization velocities u_{mf}. Although the solutions depend upon a single dimensionless parameter similar to that obtained by Caram & Hsu (1986), for clarity, we have chosen to display the results in dimensional form for $d = 1.6$ cm, with u_{mf} and Q as parameters. Figure 12 shows the results of such a parametric study. The curve for $u_{\mathrm{mf}} = 0$ corresponds to no leakage of gas into the emulsion phase, and is given by the analytical formula [2] above. The other

curves show the effect of gas leakage, which in general leads to higher pinching frequencies at a given flow rate.

We have carried out a series of such calculations, using a gap width, d, appropriate to our apparatus, values of u_{mf} appropriate to the particles listed in table 1, for a range of flow rates, Q, appropriate to the experimental range. For each particle type, this results in predictions of f vs Q, and these are shown as --- curves in figures 8–10. It is generally seen that in spite of considerable scatter in the data, the leakage model results in an improved agreement between theory and experiment for the larger particles, where gas leakage into the emulsion phase might be considered to be more important.

5. CONCLUSIONS

Bubble formation from a single jet in a 2-D fluidized bed was studied using both flow visualization and a high-frequency response capacitance probe. It was found that the jet exhibited three basic flow regimes and in the first two, a pinching instability resulted in bubble formation at a characteristic frequency, and that subsequent coalescence resulted in a bubble frequency which is a simple subharmonic of this basic frequency. The probe studies were limited to the first of these regimes, and included extensive data on the dependence of this pinching frequency on jet flow rate, particle size, background gas supplied to the surrounding emulsion and axial distance. It was found that the probe studies were in agreement with the picture which emerged from the visualization studies. The background gas had little effect on the pinching frequency or mode of instability. For small particles, the pinching frequency was in good agreement with the 2-D version of a simple model due to Davidson & Harrison (1963). There was, however, a systematic deviation from the model for larger particles. A modification of the model which incorporates leakages from the jet into the emulsion at $u = u_{mf}$ explains well the trends in the data. These considerations should carry over to models of bubble formation from jets in 3-D fluidized beds.

Acknowledgements—We wish to acknowledge the Multiphase Processing Program of the NSF and the Donors of the Petroleum Research Fund of the American Chemical Society for supporting this work. We wish to thank Dr Daniel Green for his help with the capacitance probe and Professor John Grace for several helpful comments on an earlier version of this paper.

REFERENCES

CARAM, H. S. & HSU, K.-K. 1986 Bubble formation and gas leakage in fluidized beds. *Chem. Engng Sci.* **41**, 1445–1453.

DAVIDSON, J. F. & HARRISON, D. 1963 *Fluidized Particles*. Cambridge Univ. Press, Cambs.

FITZGERALD, T. 1983 Cold modeling of fluidized bed combustors. EPRI Report OS1476.

MASSIMILLA, L. 1985 Gas jets in fluidized beds. In *Fluidization*, 2nd edn (Edited by DAVIDSON, J. F., CLIFT & HARRISON, D.), pp. 133–172. Academic Press, New York.

NGUYEN, X. T. & LEUNG, L. S. 1972 A note on bubble formation at an orifice in a fluidized bed. *Chem. Engng Sci.* **27**, 1748–1750.

ROPCHAN, W. T. 1981 Ph.D. Thesis, Stanford Univ., Stanford, Calif.

ROWE, P. N., MACGILLIVRAY, H. J. & CHEESMAN, D. J. 1979 Gas discharge from an orifice into a gas fluidized bed. *Trans. Instn chem. Engrs* **57**, 194–199.

SIT, S. P. 1981 Ph.D. Dissertation, McGill Univ., Montreal, Quebec.

SIT, S. P. & GRACE, J. R. 1981 Hydrodynamics and mass transfer in the distributor zone of fluidized beds. *Proc. 2nd Wld Congr. chem. Engrs.*

YANG, W.-C., REVAY, D., ANDERSON, R. G., CHELEN, E. J., KEAIRNS, D. L. & CICERO, D. C. 1983 Fluidized phenomena in a large-scale, cold-flow model. In *Fluidization* (Edited by KUNII, D. & TOEI, R.), pp. 77–84. Kashikojima, Japan.

YANG, W.-C., ETTEHADIEH, B., ANESTIS, T. C., GIZZIE, R. E. & HALDIPUR, G. B. 1986 Fluidization phenomenon in a large jetting fluidized bed. In *Fluidization*, 2nd edn (Edited by OSTERGAARD & SORENSEN), pp. 95–102. Academic Press, New York.

ZENZ, F. 1968 Bubble formation and grid design. *Instn Chem. Engrs (Lond.) Symp. Ser.* **30**, 136–139.

ZENZ, F. 1971 Regimes of fluidized behaviour. In *Fluidization* (Edited by DAVIDSON, J. F. & HARRISON, D.). Academic Press, New York.